

group for CRC [3–5]. However, appropriate animal models to evaluate hypertension-related colorectal carcinogenesis have not yet been generated.

To our knowledge, the present study provides the first evidence that after administration of AOM, SHRSP and SHRSP-ZF rats, both of which present with hypertension, more readily develop colonic preneoplastic lesions than normotensive WKY rats. In particular, we found that SHRSP rats experience accelerated development of ACF. This is significant because these rats did not exhibit insulin resistance, hyperleptinemia, or dyslipidemia and did not have increased adipose tissue, which are involved in the pathophysiology thought to link Mets to CRC [5–8]. These findings, therefore, suggest that hypertension *per se* might play a critical role in the early events of colorectal carcinogenesis. We have found that the angiotensin converting enzyme inhibitor captopril, an anti-hypertensive drug, significantly prevents the development of ACF in SHRSP-ZF rats [19]. These findings also support our hypothesis that blood pressure elevation *per se* might be directly involved in the early stage of colorectal carcinogenesis. However, in order to test this hypothesis, further studies are needed to establish whether other anti-hypertensive agents, such as AT-II type 1 receptor blockers and calcium channel blockers, can suppress the development of ACF by lowering blood pressure.

Among the pathophysiological disorders associated with hypertension, an increased level of oxidative stress is thought to be particularly important in CRC development [5,6]. Oxidative stress, defined as the overproduction of oxygen species combined with inadequate anti-oxidative defense mechanisms, can result in DNA damage and, consequently, mutations associated with colorectal carcinogenesis [5,20]. In the present study, the hypertensive SHRSP and SHRSP-ZF rats had significantly elevated urine 8-OHdG levels and serum d-ROM levels, which are associated with increased oxidative stress [21]. However, they also had reduced *GPx* and *CAT* mRNA levels, both of which encode antioxidant enzymes, in the colonic epithelium. These findings indicate that both SHRSP and SHRSP-ZF rats are subjected to strong oxidative stress, which might contribute to the development of ACF.

In addition to oxidative stress, the induction of chronic inflammation is also considered to play a critical role in obesity-, diabetes-, and hypertension-related colorectal carcinogenesis [5,6]. In the present study, serum levels of TNF- α and IL-6, as well as colonic expression of *MCP-1* and *iNOS* mRNA, were markedly elevated in SHRSP-ZF obese and diabetic rats. These changes might have been associated with the increase in adipose tissue in SHRSP-ZF rats because excess adipose tissue plays an important role in the exacerbation of systemic inflammation [22,23]. Furthermore, colonic epithelial expression of *TNF- α* mRNA and serum levels of COX-2 were significantly higher in both the hypertensive SHRSP and SHRSP-ZF rats, although the former did not become obese or develop diabetes. These findings are also significant because the dysregulation of TNF- α , a central mediator of chronic inflammatory diseases, and COX-2 have key roles in the stimulation of tumor growth and the progression of carcinogenesis in several tissues, including the colon and rectum [24,25].

Why did the SHRSP rats, which did not exhibit obesity and insulin resistance, experience an acceleration of oxidative stress, exacerbation of chronic inflammation, and development of ACF to the same extent as SHRSP-ZF rats that are both obese and diabetic? One possible explanation is that the dose of AOM (20 mg/kg body weight) used in the present protocol was considerably greater than that needed to induce ACF development in these hypertensive rats. A lower dose of AOM may therefore result in differences in both the number and size of ACF between SHRSP and SHRSP-ZF rats. It is also possible that an increase in the serum level of AT-II, which is the main effector peptide of the

renin-angiotensin system [12,13], might contribute to these phenomena because renin-angiotensin system activation has been implicated in the increase in oxidative stress and the induction of inflammation [11,14,26,27]. Renin-angiotensin system activation induces adipocyte inflammation, as demonstrated by the increased expression of TNF- α and IL-6 in adipose tissue, which in turn is implicated in hypertension [28,29]. In prostate cancer, treatment with AT-II stimulates the secretion of IL-6 and MCP-1 from prostate stromal cells and is associated with the increased proliferation of prostate cancer cells [30]. AT-II also induces the expression of iNOS, an inflammatory marker, along with 8-OHdG in prostate cancer cells [31], suggesting a crosslink between renin-angiotensin system-related inflammation and oxidative stress in cancer tissue.

To date, there is no definitive evidence demonstrating the effectiveness of renin-angiotensin system inhibitors in preventing human malignancies, including CRC, in hypertensive patients [32–35]. However, our findings suggest that targeting hypertension-related metabolic abnormalities, including oxidative stress and chronic inflammation caused by renin-angiotensin system activation, may be an effective strategy to prevent CRC development in patients with Mets, especially those with hypertension. In malignant tissue such as CRC, dysregulation of the renin-angiotensin system is implicated in cancer cell migration, invasion, and metastasis [10,11,13,14,36]. A recent study also showed that treatment with renin-angiotensin system inhibitors could inhibit chemically induced colorectal carcinogenesis in obese and diabetic mice by attenuating chronic inflammation and oxidative stress [37]. In order to test the potential efficacy of renin-angiotensin system inhibitors in preventing CRC development in patients with Mets, additional long-term experiments to evaluate whether these agents can prevent colorectal carcinogenesis in hypertensive rats should be conducted.

3. Experimental Section

3.1. Animals and Chemicals

Five-week-old male SHRSP, SHRSP-ZF, and WKY rats were obtained from Japan SLC (Shizuoka, Japan) and humanely maintained at Gifu University Life Science Research Center in accordance with the Institutional Animal Care Guidelines. The WKY rats are normotensive and not prone to obesity, and thus served as the control group in this study. AOM, which is widely used to mimic sporadic colon carcinogenesis by causing DNA mutations and activating several oncogenic pathways, including the K-*ras* pathway [38,39], was purchased from Wako (Osaka, Japan).

3.2. Experimental Procedure

After 1 week of acclimatization, the 6-week-old rats were divided into 3 groups of 8 rats each. All rats received an intraperitoneal injection of AOM (20 mg/kg body weight) once a week for 2 weeks. The experimental protocol and dose of AOM were based on previous studies using F344, Sprague-Dawley, or Wister rat strains [40,41]. We did not include non-AOM treated WKY rats as negative controls because no ACF was found to develop in these animals in a preliminary experiment. At the end of the experiment (2 weeks after the last injection of AOM), when the rats were 10 weeks of age, systolic and diastolic blood pressures were measured noninvasively using a tail cuff (SOFTRON BP98A; Softron, Tokyo, Japan). All rats were euthanized by CO₂ asphyxiation for colon resection. The third portion of

the excised colons (cecum side) was used to extract RNA, and the remaining part was used to determine the number of ACF [42].

3.3. Enumeration of ACF

The frequency of AOM-induced colonic premalignant lesions, ACF, was determined as previously described [42]. Briefly, the colon samples were fixed with 10% buffered formalin, stained with methylene blue (0.5% in distilled water) for 20 s, and then placed on microscope slides to count the number of ACF. The number of ACF was recorded along with the number of ACs in each focus. The data are expressed per unit area (cm²).

3.4. RNA Extraction and Quantitative Real-Time Reverse Transcription-Polymerase Chain Reaction Analysis

The epithelial crypts were isolated from colonic tissue [41]. Total RNA was then extracted from the isolated epithelial crypts using the RNAqueous-4PCR kit (Ambion Applied Biosystems, Austin, TX, USA). cDNA was amplified from 0.2 µg of total RNA using the SuperScript III First-Strand Synthesis System (Invitrogen, Carlsbad, CA, USA). Quantitative real-time reverse transcription-PCR (RT-PCR) analysis was performed using specific primers that amplify *TNF-α*, *MCP-1*, *iNOS*, *GPx*, *CAT*, and glyceraldehyde-3-phosphate dehydrogenase (*GAPDH*) genes. The sequences of these primers, which were obtained from Primer-BLAST [43], are listed in Table S1. Each sample was analyzed on a LightCycler Nano (Roche Diagnostics, Basel, Switzerland) using FastStart Essential DNA Green Master (Roche Diagnostics). Parallel amplification of *GAPDH* was used as the internal control.

3.5. Clinical Biochemistry

Blood samples from the inferior vena cava were used for chemical analyses. These samples were obtained at the time of euthanasia, prior to which the rats had fasted for 6 h. The serum levels of TNF-α (R&D Systems, Minneapolis, MN, USA), IL-6 (R & D Systems), insulin (Shibayagi, Gunma, Japan), glucose (BioVision Research Products, Mountain View, CA, USA), leptin (Shibayagi), triglyceride (Wako), NEFA (Wako), AT-II (Phoenix Pharmaceuticals, INC, Burlingame, CA, USA), and COX-2 (MyBioSource, San Diego, CA, USA) were determined using an enzyme-linked immunosorbent assay (ELISA) kit according to the manufacturer instructions.

3.6. Oxidative Stress Analysis

Urine 8-OHdG levels were determined using an ELISA kit (NIKKEN SEIL, Shizuoka, Japan). Serum levels of hydroperoxide, a marker for oxidative stress, were evaluated using the d-ROM test (FREE Carpe Diem; Diacron s.r.l., Grosseto, Italy) [21].

3.7. Statistical Analysis

All data are presented as mean ± SD and were analyzed using the GraphPad InStat software program version 3.05 (GraphPad Software, San Diego, CA, USA) for Macintosh. One-way analysis of variance

(ANOVA) was used to compare groups. If the ANOVA analysis indicated significant differences, the Tukey-Kramer multiple comparisons test was performed to compare the mean values among the groups. The differences were considered significant when the two-sided p value was less than 0.05.

4. Conclusions

The results of this study indicate that the development of AOM-induced colonic preneoplastic lesions was significantly accelerated in hypertensive rats compared to normotensive rats. This was associated with hypertension-related renin-angiotensin system activation and subsequent induction of oxidative stress and inflammation, suggesting that hypertension plays a critical role in the early stages of CRC.

Conflict of Interest

The authors declare no conflict of interest.

References

1. Alberti, K.G.; Zimmet, P.; Shaw, J.; IDF Epidemiology Task Force Consensus Group. The metabolic syndrome—A new worldwide definition. *Lancet* **2005**, *366*, 1059–1062.
2. Grundy, S.M.; Cleeman, J.I.; Daniels, S.R.; Donato, K.A.; Eckel, R.H.; Franklin, B.A.; Gordon, D.J.; Krauss, R.M.; Savage, P.J.; Smith, S.C., Jr.; *et al.* Diagnosis and management of the metabolic syndrome: An American Heart Association/National Heart, Lung, and Blood Institute Scientific Statement. *Circulation* **2005**, *112*, 2735–2752.
3. Ahmed, R.L.; Schmitz, K.H.; Anderson, K.E.; Rosamond, W.D.; Folsom, A.R. The metabolic syndrome and risk of incident colorectal cancer. *Cancer* **2006**, *107*, 28–36.
4. Stocks, T.; van Hemelrijck, M.; Manjer, J.; Bjorge, T.; Ulmer, H.; Hallmans, G.; Lindkvist, B.; Selmer, R.; Nagel, G.; Tretli, S.; *et al.* Blood pressure and risk of cancer incidence and mortality in the Metabolic Syndrome and Cancer Project. *Hypertension* **2012**, *59*, 802–810.
5. Ishino, K.; Mutoh, M.; Totsuka, Y.; Nakagama, H. Metabolic syndrome: A novel high-risk state for colorectal cancer. *Cancer Lett.* **2012**, doi:10.1016/j.canlet.2012.10.01.
6. Shimizu, M.; Kubota, M.; Tanaka, T.; Moriwaki, H. Nutraceutical approach for preventing obesity-related colorectal and liver carcinogenesis. *Int. J. Mol. Sci.* **2012**, *13*, 579–595.
7. Yuhara, H.; Steinmaus, C.; Cohen, S.E.; Corley, D.A.; Tei, Y.; Buffler, P.A. Is diabetes mellitus an independent risk factor for colon cancer and rectal cancer? *Am. J. Gastroenterol.* **2011**, *106*, 1911–1921.
8. Donohoe, C.L.; Pidgeon, G.P.; Lysaght, J.; Reynolds, J.V. Obesity and gastrointestinal cancer. *Br. J. Surg.* **2010**, *97*, 628–642.
9. De Kloet, A.D.; Krause, E.G.; Woods, S.C. The renin angiotensin system and the metabolic syndrome. *Physiol. Behav.* **2010**, *100*, 525–534.
10. Ager, E.I.; Neo, J.; Christophi, C. The renin-angiotensin system and malignancy. *Carcinogenesis* **2008**, *29*, 1675–1684.
11. Deshayes, F.; Nahmias, C. Angiotensin receptors: A new role in cancer? *Trends Endocrinol. Metab.* **2005**, *16*, 293–299.

12. Paul, M.; Poyan Mehr, A.; Kreutz, R. Physiology of local renin-angiotensin systems. *Physiol. Rev.* **2006**, *86*, 747–803.
13. Fyhrquist, F.; Saijonmaa, O. Renin-angiotensin system revisited. *J. Intern. Med.* **2008**, *264*, 224–236.
14. George, A.J.; Thomas, W.G.; Hannan, R.D. The renin-angiotensin system and cancer: Old dog, new tricks. *Nat. Rev. Cancer* **2010**, *10*, 745–759.
15. Hiraoka-Yamamoto, J.; Nara, Y.; Yasui, N.; Onobayashi, Y.; Tsuchikura, S.; Ikeda, K. Establishment of a new animal model of metabolic syndrome: SHRSP fatty (fa/fa) rats. *Clin. Exp. Pharmacol. Physiol.* **2004**, *31*, 107–109.
16. Ueno, T.; Takagi, H.; Fukuda, N.; Takahashi, A.; Yao, E.H.; Mitsumata, M.; Hiraoka-Yamamoto, J.; Ikeda, K.; Matsumoto, K.; Yamori, Y. Cardiovascular remodeling and metabolic abnormalities in SHRSP.Z-Lepr(fa)/IzmDmcr rats as a new model of metabolic syndrome. *Hypertens. Res. Off. J. Jpn. Soc. Hypertens.* **2008**, *31*, 1021–1031.
17. Chen, H.; Sullivan, G.; Yue, L.Q.; Katz, A.; Quon, M.J. QUICKI is a useful index of insulin sensitivity in subjects with hypertension. *Am. J. Physiol. Endocrinol. Metab.* **2003**, *284*, E804–E812.
18. Chrysant, S.G.; Chrysant, G.S.; Chrysant, C.; Shiraz, M. The treatment of cardiovascular disease continuum: Focus on prevention and RAS blockade. *Curr. Clin. Pharmacol.* **2010**, *5*, 89–95.
19. Kochi, K.; Shimizu, M.; Ohno, T.; Baba, A.; Sumi, T.; Kubota, M.; Shirakami, Y.; Tsurumi, H.; Tanaka, T.; Moriwaki, H. Department of Internal Medicine, Gifu University Graduate School of Medicine, 2013, Unpublished data.
20. Tudek, B.; Speina, E. Oxidatively damaged DNA and its repair in colon carcinogenesis. *Mutat. Res.* **2012**, *736*, 82–92.
21. Suzuki, Y.; Imai, K.; Takai, K.; Hanai, T.; Hayashi, H.; Naiki, T.; Nishigaki, Y.; Tomita, E.; Shimizu, M.; Moriwaki, H. Hepatocellular carcinoma patients with increased oxidative stress levels are prone to recurrence after curative treatment: A prospective case series study using the d-ROM test. *J. Cancer Res. Clin. Oncol.* **2013**, in press.
22. Hotamisligil, G.S.; Shargill, N.S.; Spiegelman, B.M. Adipose expression of tumor necrosis factor- α : Direct role in obesity-linked insulin resistance. *Science* **1993**, *259*, 87–91.
23. Hotamisligil, G.S. Inflammation and metabolic disorders. *Nature* **2006**, *444*, 860–867.
24. Szlosarek, P.; Charles, K.A.; Balkwill, F.R. Tumour necrosis factor- α as a tumour promoter. *Eur. J. Cancer* **2006**, *42*, 745–750.
25. Gupta, R.A.; Dubois, R.N. Colorectal cancer prevention and treatment by inhibition of cyclooxygenase-2. *Nat. Rev. Cancer* **2001**, *1*, 11–21.
26. Cassis, P.; Conti, S.; Remuzzi, G.; Benigni, A. Angiotensin receptors as determinants of life span. *Pflügers Arch.* **2010**, *459*, 325–332.
27. Smith, G.R.; Missailidis, S. Cancer, inflammation and the AT1 and AT2 receptors. *J. Inflamm.* **2004**, *1*, 3.
28. Massiera, F.; Bloch-Faure, M.; Ceiler, D.; Murakami, K.; Fukamizu, A.; Gasc, J.M.; Quignard-Boulange, A.; Negrel, R.; Ailhaud, G.; Seydoux, J.; *et al.* Adipose angiotensinogen is involved in adipose tissue growth and blood pressure regulation. *FASEB* **2001**, *15*, 2727–2729.
29. Yvan-Charvet, L.; Massiera, F.; Lamande, N.; Ailhaud, G.; Teboul, M.; Moustaid-Moussa, N.; Gasc, J.M.; Quignard-Boulange, A. Deficiency of angiotensin type 2 receptor rescues obesity but not hypertension induced by overexpression of angiotensinogen in adipose tissue. *Endocrinology* **2009**, *150*, 1421–1428.

30. Uemura, H.; Ishiguro, H.; Nagashima, Y.; Sasaki, T.; Nakaigawa, N.; Hasumi, H.; Kato, S.; Kubota, Y. Antiproliferative activity of angiotensin II receptor blocker through cross-talk between stromal and epithelial prostate cancer cells. *Mol. Cancer Ther.* **2005**, *4*, 1699–1709.
31. Uemura, H.; Ishiguro, H.; Ishiguro, Y.; Hoshino, K.; Takahashi, S.; Kubota, Y. Angiotensin II induces oxidative stress in prostate cancer. *Mol. Cancer Res. MCR* **2008**, *6*, 250–258.
32. Lever, A.F.; Hole, D.J.; Gillis, C.R.; McCallum, I.R.; McInnes, G.T.; MacKinnon, P.L.; Meredith, P.A.; Murray, L.S.; Reid, J.L.; Robertson, J.W. Do inhibitors of angiotensin-I-converting enzyme protect against risk of cancer? *Lancet* **1998**, *352*, 179–184.
33. Lang, L. ACE inhibitors may reduce esophageal cancer incidence. *Gastroenterology* **2006**, *131*, 343–344.
34. Sipahi, I.; Chou, J.; Mishra, P.; Debanne, S.M.; Simon, D.I.; Fang, J.C. Meta-analysis of randomized controlled trials on effect of angiotensin-converting enzyme inhibitors on cancer risk. *Am. J. Cardiol.* **2011**, *108*, 294–301.
35. Hallas, J.; Christensen, R.; Andersen, M.; Friis, S.; Bjerrum, L. Long term use of drugs affecting the renin-angiotensin system and the risk of cancer: A population-based case-control study. *Br. J. Clin. Pharmacol.* **2012**, *74*, 180–188.
36. Shimomoto, T.; Ohmori, H.; Luo, Y.; Chihara, Y.; Denda, A.; Sasahira, T.; Tatsumoto, N.; Fujii, K.; Kuniyasu, H. Diabetes-associated angiotensin activation enhances liver metastasis of colon cancer. *Clin. Exp. Metast.* **2012**, *29*, 915–925.
37. Kubota, M.; Shimizu, M.; Sakai, H.; Yasuda, Y.; Ohno, T.; Kochi, T.; Tsurumi, H.; Tanaka, T.; Moriwaki, H. Renin-angiotensin system inhibitors suppress azoxymethane-induced colonic preneoplastic lesions in C57BL/KsJ-db/db obese mice. *Biochem. Biophys. Res. Commun.* **2011**, *410*, 108–113.
38. Takahashi, M.; Wakabayashi, K. Gene mutations and altered gene expression in azoxymethane-induced colon carcinogenesis in rodents. *Cancer Sci.* **2004**, *95*, 475–480.
39. Chen, J.; Huang, X.F. The signal pathways in azoxymethane-induced colon cancer and preventive implications. *Cancer Biol. Ther.* **2009**, *8*, 1313–1317.
40. Reddy, B.S. Studies with the azoxymethane-rat preclinical model for assessing colon tumor development and chemoprevention. *Environ. Mol. Mutagenesis* **2004**, *44*, 26–35.
41. Raju, J. Azoxymethane-induced rat aberrant crypt foci: Relevance in studying chemoprevention of colon cancer. *World J. Gastroenterol.* **2008**, *14*, 6632–6635.
42. Ogawa, K.; Hara, T.; Shimizu, M.; Ninomiya, S.; Nagano, J.; Sakai, H.; Hoshi, M.; Ito, H.; Tsurumi, H.; Saito, K.; *et al.* Suppression of azoxymethane-induced colonic preneoplastic lesions in rats by 1-methyltryptophan, an inhibitor of indoleamine 2,3-dioxygenase. *Cancer Sci.* **2012**, *103*, 951–918.
43. Primer Blast. Available online: <http://www.ncbi.nlm.nih.gov/tools/primer-blast/> (accessed on 12 July 2012).

© 2013 by the authors; licensee MDPI, Basel, Switzerland. This article is an open access article distributed under the terms and conditions of the Creative Commons Attribution license (<http://creativecommons.org/licenses/by/3.0/>).

Effects of Indoleamine 2,3-Dioxygenase Deficiency on High-Fat Diet-Induced Hepatic Inflammation

Junji Nagano¹, Masahito Shimizu^{1*}, Takeshi Hara¹, Yohei Shirakami², Takahiro Kochi¹, Nobuhiko Nakamura¹, Hirofumi Ohtaki², Hiroyasu Ito², Takuji Tanaka³, Hisashi Tsurumi¹, Kuniaki Saito⁴, Mitsuru Seishima², Hisataka Moriwaki¹

1 Department of Internal Medicine, Gifu University Graduate School of Medicine, Gifu, Japan, **2** Department of Informative Clinical Medicine, Gifu University Graduate School of Medicine, Gifu, Japan, **3** Department of Tumor Pathology, Gifu University Graduate School of Medicine, Gifu, Japan, **4** Human Health Sciences, Graduate School of Medicine and Faculty of Medicine, Kyoto University, Kyoto, Japan

Abstract

Hepatic immune regulation is associated with the progression from simple steatosis to non-alcoholic steatohepatitis, a severe condition of inflamed fatty liver. Indoleamine 2,3-dioxygenase (IDO), an intracellular enzyme that mediates the catabolism of L-tryptophan to L-kynurenine, plays an important role in hepatic immune regulation. In the present study, we examined the effects of IDO gene silencing on high-fat diet (HFD)-induced liver inflammation and fibrosis in mice. After being fed a HFD for 26 weeks, the IDO-knockout (KO) mice showed a marked infiltration of inflammatory cells, especially macrophages and T lymphocytes, in the liver. The expression levels of F4/80, IFN γ , IL-1 β , and IL-6 mRNA in the liver and the expression levels of F4/80 and TNF- α mRNA in the white adipose tissue were significantly increased in IDO-KO mice, although hepatic steatosis, the accumulation of intrahepatic triglycerides, and the amount of oxidative stress were lower than those in IDO-wild-type mice. IDO-KO mice also developed marked pericellular fibrosis in the liver, accumulated hepatic hydroxyproline, and exhibited increased expression levels of hepatic TGF- β 1 mRNA. These findings suggest that IDO-KO renders the mice more susceptible to HFD-induced hepatic inflammation and fibrosis. Therefore, IDO may have a protective effect against hepatic fibrosis, at least in this HFD-induced liver injury model.

Citation: Nagano J, Shimizu M, Hara T, Shirakami Y, Kochi T, et al. (2013) Effects of Indoleamine 2,3-Dioxygenase Deficiency on High-Fat Diet-Induced Hepatic Inflammation. PLoS ONE 8(9): e73404. doi:10.1371/journal.pone.0073404

Editor: Rafael Aldabe, Centro de Investigación en Medicina Aplicada (CIMA), Spain

Received: February 18, 2013; **Accepted:** July 23, 2013; **Published:** September 9, 2013

Copyright: © 2013 Nagano et al. This is an open-access article distributed under the terms of the Creative Commons Attribution License, which permits unrestricted use, distribution, and reproduction in any medium, provided the original author and source are credited.

Funding: These authors have no support or funding to report.

Competing interests: The authors have declared that no competing interests exist.

* E-mail: shimim-gif@umin.ac.jp

Introduction

Non-alcoholic fatty liver disease (NAFLD), which is strongly associated with obesity and metabolic syndrome, is one of the most common causes of chronic liver disease worldwide. NAFLD includes a spectrum of disturbances that encompasses various degrees of liver damage ranging from non-alcoholic steatohepatitis (NASH), a severe condition of inflamed fatty liver that can progress to hepatic fibrosis, cirrhosis, or even hepatocellular carcinoma. The critical features of NASH, in addition to simple steatosis, include forms of hepatocellular degeneration such as ballooning and Mallory hyaline degeneration, mixed inflammatory cell infiltration, and the development of fibrosis [1,2]. Obesity is associated with chronic low-grade systemic inflammation, which contributes to the progression from hepatic steatosis to NASH [3]. Among various immune cells, T lymphocytes play a critical role in the induction of inflammation both in the liver and in white adipose tissue

(WAT) [4,5]. Macrophage infiltration into WAT is also an early contributing event in the development of systemic inflammation because it is accompanied by tumor necrosis factor (TNF)- α production, a central mediator of the inflammatory response [6]. These reports, therefore, indicate that chronic inflammation plays a key role in the pathogenesis of NASH [7].

Indoleamine 2,3-dioxygenase (IDO), an intracellular enzyme that degrades the essential amino acid L-tryptophan along the L-kynurenine pathway, is induced during inflammation by several immune factors, including interferon (IFN) γ [8]. IDO is considered to exert powerful immunomodulatory effects, including the promotion of immune tolerance, because L-kynurenine and some other metabolites derived from tryptophan by IDO can inhibit T cell activation and proliferation while increasing immunosuppressive regulatory T-cell (Tregs) activity [9–11]. The liver is a special lymphoid organ and is thus particularly susceptible to injury as a result of the immune response, which is primarily mediated by T lymphocytes [12].

IDO is activated in infectious, autoimmune, and malignant diseases that involve cellular immune activation in various organs, including the liver [13]. In fact, upregulation of the IDO expression in the liver and increased serum IDO activity have been found in chronic hepatitis C patients [14,15]. The IDO expression is also enhanced in the liver and adipose tissue in obese individuals [16].

Several rodent studies have revealed the role of IDO in liver injury. In hepatitis B virus (HBV) transgenic mice, the IDO expression in hepatocytes is enhanced in mice with liver injury caused by HBV-specific cytotoxic T lymphocytes [17]. Inhibition of IDO activity exacerbates liver injury in both α -galactosylceramide- and carbon tetrachloride (CCl₄)-induced acute hepatitis models and is associated with the induction of TNF- α [18,19]. These reports suggest that IDO plays a critical role in the regulation of liver inflammation and that targeting IDO activity might be an effective strategy for attenuating acute liver injury. However, the role of IDO in steatosis-induced liver injury has not yet been clarified. In the present study, we examined the effects of IDO on high-fat diet (HFD)-induced liver steatosis and subsequent hepatic inflammation and fibrosis using IDO-deficient mice.

Materials and Methods

2.1 Animals and experimental procedure

This study was carried out in strict accordance with the recommendations of the Guide for the Care and Use of Laboratory Animals of Gifu University Life Science Research Center. The protocol was approved by the Committee on the Ethics of Animal Experiments of Gifu University (Permit Number: 24-65). All surgeries were performed under sodium pentobarbital anesthesia, and all efforts were made to minimize animal suffering. Five-week-old male IDO-wild-type (WT) mice and IDO-knockout (KO) mice with a C57BL/6J background were obtained from The Jackson Laboratory (Bar Harbor, ME, USA). HFD-60 (506.2 kcal/100 g) with 62.2% of the calories derived from fat was purchased from Oriental Yeast (Tokyo, Japan). The cholesterol content of the diet was 33.0 mg/100 g. After 1 week of acclimatization, 8 WT mice and 8 KO mice were given a pelleted HFD throughout the experiment (26 weeks) with free access to tap water and food. At the end of the experiment (32 weeks of age), all mice were sacrificed under sodium pentobarbital anesthesia and the livers were carefully removed.

2.2 Histopathological and immunohistochemical examinations

For all the experimental mice, 4 μ m-thick sections of formalin-fixed and paraffin-embedded livers were stained with hematoxylin & eosin (H&E) for conventional histopathology or with Sirius Red stain to determine the presence of liver fibrosis. The histological features of the livers were evaluated using the NAFLD activity score (NAS) system [20]. The computer-assisted quantitative analyses of hepatic fibrosis development were carried out using the BZ-Analyzer-II software program (KEYENCE, Osaka, Japan) [21,22].

In order to evaluate the infiltration of inflammatory cells in the liver, immunohistochemical staining for Mac-1 (a macrophage marker), CD3 (a T-cell marker), and NIMP-R14 (a neutrophil marker) of paraffin-embedded sections was performed using the linked streptavidin-biotin method. Rat monoclonal anti-Mac-1 antibody (MAB1387Z, 1:50 dilution) was purchased from Chemicon International (Temecula, CA, USA). Rabbit polyclonal anti-CD3 (ab5690, 1:100 dilution) antibodies and rat monoclonal anti-neutrophil antibody (NIMP-R14, ab2557, 1:50 dilution) were obtained from Abcam (Cambridge, MA, USA). On the Mac-1-, CD3-, and NIMP-R14-immunostained sections, the inflammatory cells that intensively reacted to these antibodies were counted and the data are expressed as the percentage of total inflammatory cells in the liver. A positive cell index (%) was determined by counting at least 500 cells in a section from each mouse.

2.3 Hepatic hydroxyproline analysis

The hepatic hydroxyproline content (μ mol/g wet liver) was quantified colorimetrically in duplicate samples from approximately 200mg of the wet-weight liver tissues, as described previously [22].

2.4 RNA extraction and quantitative real-time RT-PCR analysis

Total RNA was isolated from the livers and adipose tissue of the mice using the RNeasy Mini Kit and RNeasy Lipid Tissue Mini Kit (Qiagen, Hilden, Germany), respectively [21]. cDNA was amplified from 0.5 μ g of total RNA using the SuperScript III First-Strand Synthesis System (Invitrogen, Carlsbad, CA, USA). A quantitative real-time reverse transcription-PCR (RT-PCR) analysis was performed using specific primers that amplify F4/80, IFN γ , interleukin (IL)-1 β , IL-6, TNF- α , superoxide dismutase (SOD)-1, SOD-2, glutathione peroxidase (GPx), transforming growth factor (TGF)- β 1, glyceraldehyde-3-phosphate dehydrogenase (GAPDH), and the ribosomal protein large P0 (RPLP0) genes. The sequences of the primers for these genes, which were obtained from Universal ProbeLibrary Assay Design Center (Roche, Indianapolis, IN, USA), are shown in Table 1. The analysis to quantify the expression levels of tryptophan 2,3-dioxygenase (TDO) was performed using TaqMan Gene Expression Assays (Applied Biosystems, Foster City, CA, USA) and TOYOBO Real-time PCR Master Mix (TOYOBO, Osaka, Japan), as described previously [23]. Each sample was analyzed on a LightCycler Nano (Roche) with FastStart Essential DNA Green Master (Roche). The parallel amplification of GAPDH and RPLP0 was used as the internal control for liver and adipose tissue, respectively.

2.5 Clinical chemistry

The serum levels of alanine aminotransferase (ALT) were measured using a standard clinical automatic analyzer (type 7180; Hitachi, Tokyo, Japan).

Table 1. Primer sequences.

Gene	Primer sequence
SOD1	F 5'- CAGGACCTCATTTTAATCCTCAC-3'
	R 5'- TGCCAGGCTCTCCAACAT-3'
SOD2	F 5'- TGCTCTAATCAGGACCCATTG-3'
	R 5'- GTAGTAAGCGTGCTCCACAC-3'
GPx	F 5'- TTTCCCGTGAATCAGTTC-3'
	R 5'- TCGGACGTACTTGAGGGAAT-3'
F4/80	F 5'- ACAAGACTGACAACCAGACGG-3'
	R 5'- TAGCATCCAGAAGAAGCAGGCGA-3'
IFN γ	F 5'- AGCAACAGCAAGGCGAAAAG-3'
	R 5'- CGTTCCTGAGGCTGGATTC-3'
IL-1 β	F 5'- CAAGCAACGACAAAATACCTGTG-3'
	R 5'- AGACAAACCGTTTTTCCATCTTCT-3'
IL-6	F 5'- CCGGAGAGGAGACTTCACAGAG-3'
	R 5'- CTGCAAGTCATCATCGTTGTT-3'
TNF- α	F 5'- TGCCCCAGACCCTCACACTCAG-3'
	R 5'- ACCCATCGGCTGGCACCCT-3'
TGF- β 1	F 5'- ACCGGAGAGCCCTGGATACCA-3'
	R 5'- TATAGGGGAGGTTCCAGACA-3'
RPLP0	F 5'- ACTGGTCTAGGACCCGAGAAG-3'
	R 5'- CTCCCACCTGTCTCCAGTC-3'
GAPDH	F 5'- GACATCAAGAAGGTGGTGAAGCAG-3'
	R 5'- ATACCAGGAAATGAGCTTGACAAA-3'

doi: 10.1371/journal.pone.0073404.t001

2.6 Oxidative stress analysis

The serum hydroperoxide levels, one of the markers of oxidative stress, were determined using the derivatives of reactive oxygen metabolites (d-ROM) test (FREE Carpe Diem; Diacron s.r.l., Grosseto, Italy), according to the manufacturer's protocol.

2.7 Determination of the enzymatic activity of IDO

The IDO activity level in the serum was determined by calculating the ratio of the L-kynurenine/L-tryptophan concentrations [23]. Serum samples were deproteinized with 3% perchloric acid. Following centrifugation, aliquots of supernatant were collected to determine the concentrations of L-tryptophan and L-kynurenine using HPLC, as described previously [18].

2.8 Hepatic lipid analysis

After total lipids were extracted from the frozen livers (approximately 200 mg), the triglyceride levels were measured using the triglyceride E-test kit (Wako, Osaka, Japan) [21].

2.9 Statistical analysis

The data are expressed as the mean \pm SD. Statistical significance of the difference between mean values was evaluated using the Mann-Whitney *U* test. Significance was defined as a *P* value less than 0.05.

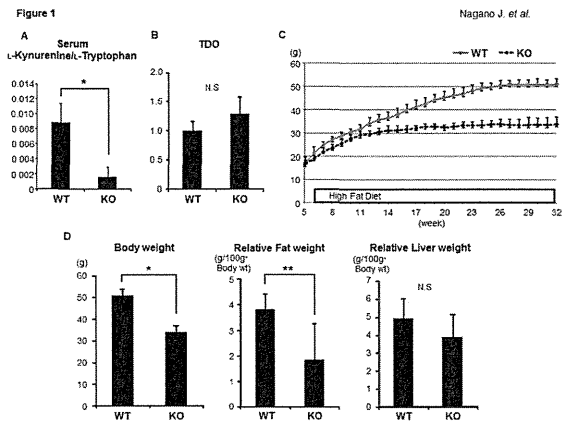


Figure 1. Effects of IDO deficiency on the serum L-kynurenine/L-tryptophan ratio, the expression levels of TDO in the liver, the growth curve, and the body, liver, and fat weights of the experimental mice. (A) The functional IDO activity level was determined by measuring the concentrations of L-kynurenine and L-tryptophan using HPLC. The L-kynurenine/L-tryptophan ratio indicates the IDO activity. (B) Total RNA was isolated from the livers of the experimental mice, and the expression levels of TDO mRNA were examined using quantitative real-time RT-PCR with specific primers. (C) The growth curve of the experimental mice. The body weights of all mice were measured once a week during the experiment. (D) The body weights and relative weights of the adipose tissues and livers of the experimental mice at the termination of the study. The values are expressed as the mean \pm SD. * *P* < 0.001, ** *P* < 0.05.

doi: 10.1371/journal.pone.0073404.g001

Results

3.1 General observations

We initially examined the enzymatic activity of IDO in the serum of the experimental mice by measuring the concentrations of L-kynurenine and L-tryptophan. The L-kynurenine/L-tryptophan ratios in serum of the IDO-KO mice were significantly lower than those in the serum of the IDO-WT mice (Figure 1A, *P* < 0.001), indicating that IDO activity was clearly inhibited in the IDO-KO mice. TDO, a hepatic enzyme that catalyses the first step of tryptophan degradation, was expressed in the liver in both the IDO-WT mice and the IDO-KO mice; however, IDO deficiency did not have a significant effect on the TDO mRNA expression (Figure 1B). Figure 1C shows the growth curves of the mice during this experiment. The body weight gain of the IDO-KO mice was smaller than that of the IDO-WT mice. At the end of the experiment, the body weights (Figure 1D, *P* < 0.001) and the relative weights of the adipose tissues of the IDO-KO mice (Figure 1D, *P* < 0.05) were also significantly lower than those of the IDO-WT mice.

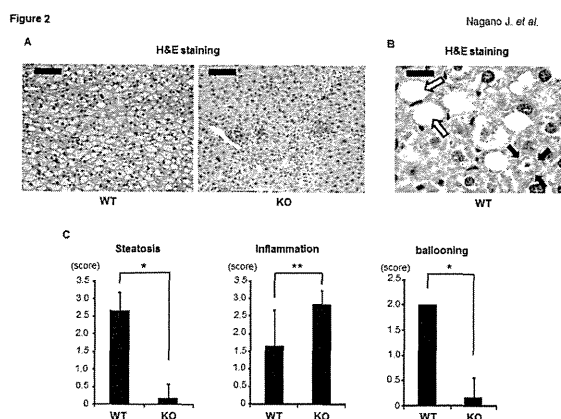


Figure 2. Effects of IDO deficiency on hepatic histopathology in the experimental mice. (A) and (B) H&E staining of liver sections from the experimental mice. (A) Representative photomicrographs of the liver sections of the IDO-WT mice and IDO-KO mice (low-power field). Black bar: 100 μ m. (B) An enlarged photo (high-power field) of the liver sections from the IDO-WT mice. Ballooned hepatocytes (indicated by white arrows) and Mallory-Denk bodies (indicated by black arrows) were observed. Black bar: 20 μ m. (C) The presence of NAS (steatosis, inflammation, and ballooning) was determined based on the histopathological analysis. The values are expressed as the mean \pm SD. * $P < 0.001$, ** $P < 0.05$.

doi: 10.1371/journal.pone.0073404.g002

3.2 Effects of IDO deficiency on hepatic histopathology in the experimental mice

The H&E staining results of the livers of the IDO-KO mice and IDO-WT mice after 26 weeks of being fed the HFD are presented in Figure 2A and B. The infiltration of inflammatory cells was markedly increased in the livers of the IDO-KO mice, and the NAS inflammation scores were significantly higher than those in the IDO-WT mice (Figure 2C, $P < 0.05$). Interestingly, the hepatic steatosis and ballooning degeneration of hepatocytes were lower in the IDO-KO mice than in the IDO-WT mice at this experimental time point (Figure 2C, $P < 0.001$). In addition to the ballooned hepatocytes, Mallory-Denk bodies, which are a recognized feature of alcoholic hepatitis and NASH [24], were also observed in the liver of IDO-WT mice (Figure 2B).

3.3 Effects of IDO deficiency on the intrahepatic triglyceride levels, the serum ALT levels, and oxidative stress in the experimental mice

The histological findings were consistent with the measured intrahepatic triglyceride contents: the levels of triglycerides in the livers of the IDO-KO mice were significantly lower than those in the livers of the IDO-WT mice (Figure 3A, $P < 0.001$). The serum levels of ALT in the IDO-KO mice were also significantly decreased relative to those in the IDO-WT mice (Figure 3B, $P < 0.01$). In addition, the serum d-ROM levels,

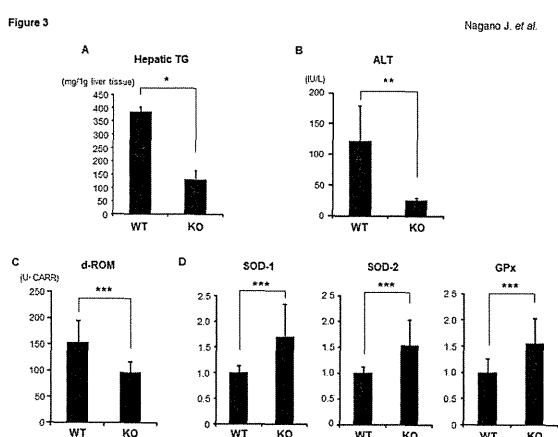


Figure 3. Effects of IDO deficiency on intrahepatic triglycerides, the serum ALT levels, and oxidative stress in the experimental mice. (A) Hepatic lipids were extracted from the frozen livers of the experimental mice, and the triglyceride levels were measured. (B) At sacrifice, blood samples were collected and the serum levels of ALT were assayed. (C) The hydroperoxide levels in the serum at the end of the experiment were determined using the d-ROM test. (D) Total RNA was isolated from the livers of the experimental mice, and the expression levels of SOD-1, SOD-2, and GPx mRNA were examined using quantitative real-time RT-PCR with specific primers. The values are expressed as the mean \pm SD. * $P < 0.001$, ** $P < 0.01$, *** $P < 0.05$.

doi: 10.1371/journal.pone.0073404.g003

which reflect the serum hydroperoxide levels, were significantly lower in the IDO-KO mice than in the IDO-WT mice (Figure 3C, $P < 0.05$). Compared to the IDO-WT mice, there were also significant increases in the expression levels of SOD-1, SOD-2, and GPx mRNA, which encode antioxidant enzymes, in the livers of the IDO-KO mice (Figure 3D, $P < 0.05$). These findings indicate that hepatic triglyceride accumulation and oxidative stress are reduced, while antioxidant activity is increased, in mice lacking the IDO gene.

3.4 Effects of IDO deficiency on inflammation in the livers and WAT of the experimental mice

We next examined the expression levels of inflammatory mediators that are implicated in the progression of fatty liver to NASH [7] in the experimental mice. A quantitative real-time RT-PCR analysis revealed that the expression levels of F4/80, a marker of macrophages, were significantly increased in the livers of the IDO-KO mice in comparison to those observed in the livers of the IDO-WT mice (Figure 4A, $P < 0.01$). There were also significant increases in the expression levels of inflammatory mediators, including IFN γ , IL-1 β , and IL-6 mRNA, in the livers of the IDO-KO mice compared to those observed in the livers of the IDO-WT mice (Figure 4A, $P < 0.05$). The expression levels of TNF- α mRNA were also higher in the livers of the IDO-KO mice than in the livers of the IDO-WT mice;

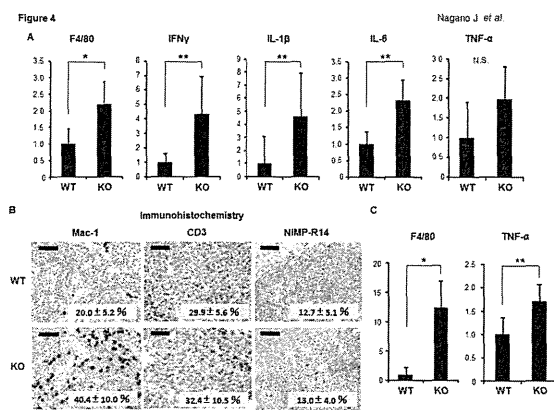


Figure 4. Effects of IDO deficiency on the inflammation in the liver and white adipose tissue of the experimental mice. (A) The expression levels of F4/80, IFN γ , IL-1 β , IL-6, and TNF- α mRNA in the livers of the experimental mice. (B) The results of the immunohistochemical analyses of Mac-1, CD3, and NIMP-R14 in the livers of the experimental mice. A positive cell index (%) was shown in each photo. Black bar: 50 μ m. (C) The expression levels of F4/80 and TNF- α mRNA in the WAT of the experimental mice. Total RNA was isolated from the livers (A) and WAT (C) of the experimental mice, and the expression levels of each mRNA were examined using quantitative real-time RT-PCR with specific primers. The expression levels of GAPDH mRNA and RPLP0 mRNA were used as internal controls for the liver and WAT, respectively. The values are expressed as the mean \pm SD. * $P < 0.01$, ** $P < 0.05$.

doi: 10.1371/journal.pone.0073404.g004

however, the difference was insignificant (Figure 4A). Furthermore, the immunohistochemical analyses demonstrated that the inflammatory cells that had infiltrated into the livers of the IDO-KO mice positively reacted with either the anti-Mac-1 (40.4 \pm 10.0%) or anti-CD3 (32.4 \pm 10.5%) antibodies. On the other hand, the infiltration of neutrophils (13.0 \pm 4.0%) was low compared to that of macrophages and T-cells. These findings suggest that macrophages and T lymphocytes were the predominantly increased cell populations in the livers of the IDO-KO mice. The infiltration of Mac-1 positive cells in the livers of IDO-KO mice (40.4 \pm 10.0%) was high compared to that of IDO-WT mice (20.0 \pm 5.2%) (Figure 4B, $P < 0.05$), and this is consistent with the results of RT-PCR analysis showing the increased levels of F4/80 mRNA in the livers of IDO-KO mice (Figure 4A).

Moreover, as shown in Figure 4C, the expression levels of F4/80 ($P < 0.01$) and TNF- α ($P < 0.05$) mRNA in WAT were both significantly increased in the IDO-KO mice compared to those observed in the IDO-WT mice, indicating that inflammation is augmented in WAT, in addition to the liver, in the IDO-KO mice [24].

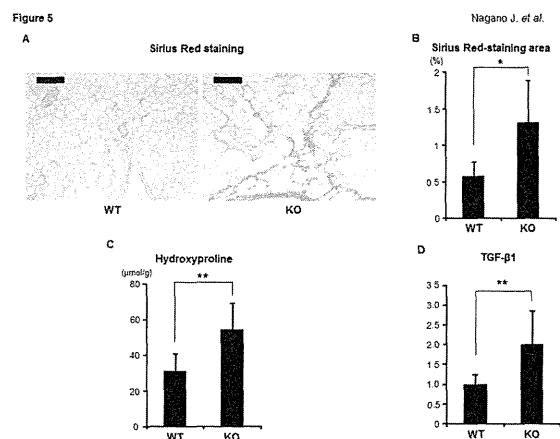


Figure 5. Effects of IDO deficiency on the hepatic fibrosis in the experimental mice. (A) Representative photomicrographs of liver sections stained with Sirius Red to show fibrosis. Black bar: 100 μ m. (B) The Sirius Red-stained images of fibrosis were analyzed using a BZ-9000 fluorescence microscope, and the fibrotic area was measured using a BZ-Analyzer-II. (C) The hepatic hydroxyproline contents were quantified colorimetrically. (D) Total RNA was isolated from the livers of the experimental mice, and the expression levels of TGF- β 1 mRNA were examined using quantitative real-time RT-PCR with specific primers. The values are expressed as the mean \pm SD. * $P < 0.01$, ** $P < 0.05$.

doi: 10.1371/journal.pone.0073404.g005

3.5 Effects of IDO deficiency on hepatic fibrosis in the experimental mice

We next examined whether IDO deficiency has an effect on the development of steatosis-induced hepatic fibrosis. An examination of Sirius Red-stained sections indicated that, compared to the IDO-WT mice, the IDO-KO mice markedly developed pericellular fibrosis in the liver (Figure 5A and B, $P < 0.01$). Similar findings were observed in the measured hepatic hydroxyproline contents: the IDO-KO mice showed a significant increase in the amount of hydroxyproline observed in the liver (Figure 5C, $P < 0.05$). The expression levels of TGF- β 1 mRNA, a central regulator of chronic liver disease contributing to fibrogenesis through inflammation [25], were also remarkably elevated in the livers of the IDO-KO mice compared to those observed in the livers of the IDO-WT mice (Figure 5D, $P < 0.05$). These findings may indicate that IDO-KO mice are susceptible to the development of steatosis-induced hepatic fibrosis.

Discussion

The results of the present study indicate that HFD-induced hepatic inflammation and fibrosis are significantly aggravated in IDO-KO mice, although the level of hepatic steatosis and amount of oxidative stress were lower compared to those in IDO-WT mice. Therefore, IDO deficiency is critically involved in

the acceleration of hepatic inflammation observed in the present study.

IDO is a rate-limiting enzyme that can degrade tryptophan via the kynurenine pathway. Because the IDO expression and its enzymatic activity, which are tightly controlled by several immune mediators such as IFN γ , play a key role in the suppression of the immune response [8–11], inhibiting the expression and activity of IDO might promote inflammatory signaling. Therefore, based on our present results, we consider that IDO-deficient mice are more susceptible to the induction of inflammation by HFD. Our results are consistent with those of recent reports showing that the inhibition of the enzymatic activity of IDO significantly exacerbated liver injury in α -galactosylceramide (α -GalCer)- and CCl $_4$ -induced acute hepatitis animal models via the upregulation of IL-6 and TNF- α [18,19]. When the IDO-KO mice were treated with α -GalCer, the production of TNF- α from the infiltrating macrophages in the liver was significantly accelerated, and thus led to the development of severe hepatitis [18]. Therefore, in the present study, the increase in the number of hepatic macrophages might have been critically involved in the exacerbation of HFD-induced hepatic inflammation in the IDO-KO mice. These reports [18,19], together with the results of the present study, suggest that IDO may play a critical role in suppressing excess induction and progression of inflammation in the liver.

Innate immune cells, including Kupffer cells, natural killer T cells, and natural killer cells, play important roles in the excessive production of hepatic T helper 1 cytokines, which is associated with the development of steatohepatitis [4]. The regulation of the immune response by IDO is predominantly based on the ability of IDO to suppress the activation of lymphocytes [9–11]. An increased IDO activity inhibits proliferation and induces apoptosis in T cells and natural killer cells via tryptophan depletion and the production of toxic tryptophan metabolites [9]. In addition, recent studies have revealed that IDO inhibits T cell activation by driving the development of Tregs [10,11]. Tregs, which are actively engaged in the negative control of a variety of immune responses, are recognized as being one of the key players in hepatic immune regulation [26]. HFD-induced steatosis in mice is associated with the depletion of hepatic Tregs and leads to upregulation of the inflammatory pathway [27]. Therefore, an IDO deficiency may increase T cell activation, either directly or indirectly, by suppressing Tregs and thus contributed to a worsening of hepatic inflammation in the present study.

Obesity is associated with systemic low-grade inflammation and immune activation [5,6]. One clinical trial reported that activation of IDO is associated with reduced plasma tryptophan levels in obese patients [28]. IDO is also overexpressed in the liver and adipose tissue in obese subjects [16]. These reports indicate that the overexpression and activation of IDO are

implicated in chronic immune activation in obese individuals. T cell infiltration into WAT and subsequent recruitment and activation of macrophages can induce TNF- α production, which is associated with the development of systemic inflammation [5,6]. The present study showed that the expression levels of F4/80 and TNF- α mRNA in WAT are elevated in IDO-KO mice compared to those observed in IDO-WT mice when the mice are fed an HFD, indicating that inflammation of WAT induced by HFD is worsened in IDO deficiency mice. Therefore, our findings suggest that IDO might have the ability to attenuate overactive immune responses caused by obesity in WAT in addition to the liver.

There are some possible limitations associated with the present study. For instance, a recent study demonstrated that neither the overexpression of IDO nor inhibition of its enzymatic activity affected the lipid accumulation in the liver, although the combination of L-tryptophan treatment and a high fat and high fructose diet exacerbated the hepatic steatosis [29]. Therefore, further experiments will be required to clarify the role of IDO and the L-kynurenine/L-tryptophan pathway in the development of hepatic steatosis. Furthermore, after 26 weeks of being fed the HFD, the IDO-KO mice showed lower steatosis and oxidative stress than the IDO-WT mice. The hepatocyte ballooning, which indicates hepatocyte injury, was also decreased in IDO-KO mice compared to IDO-WT mice. These findings seem paradoxical given the enhanced inflammation and fibrosis in IDO-KO mice in response to the HFD. A possible explanation might be that the liver inflammation proceeded earlier in IDO-KO mice, in a similar manner to NAFLD in the clinical setting, where many cases with NAFLD show the disappearance of steatosis during its natural history, while exhibiting severe fibrosis and cirrhosis in the late stages [30,31]. In order to verify this possibility, time course studies that evaluate the levels of hepatic injury, steatosis, and inflammation caused by HFD in the early phase should be conducted. In addition, a recent study revealed that hepatic fat deposits were broken down to provide energy for fibrogenesis in a CCl $_4$ -treated mouse model [32]. Such a mechanism might have also been active in our HFD-fed IDO-KO mice, but again, further experiments will be required to confirm this hypothesis.

In conclusion, we herein demonstrated that IDO deficiency worsens hepatic and WAT inflammation in mice fed an HFD. Our findings suggest that regulation of the IDO-mediated immune response might be an interesting strategy for managing steatosis-related hepatic injury.

Author Contributions

Performed the experiments: JN YS TK NN HO. Analyzed the data: JN MS TT. Wrote the manuscript: JN MS TH HI TT HT KS MS HM.

References

- Angulo P (2002) Nonalcoholic fatty liver disease. *N Engl J Med* 346: 1221-1231. doi:10.1056/NEJMra011775. PubMed: 11961152.
- Farrell GC, Larter CZ (2006) Nonalcoholic fatty liver disease: from steatosis to cirrhosis. *Hepatology* 43: S99-S112. doi:10.1002/hep.20973. PubMed: 16447287.
- Cusi K (2012) Role of obesity and lipotoxicity in the development of nonalcoholic steatohepatitis: pathophysiology and clinical implications. *Gastroenterology* 142: 711-725 e716. doi:10.1053/j.gastro.2012.02.003. PubMed: 22326434.
- Zhan YT, An W (2010) Roles of liver innate immune cells in nonalcoholic fatty liver disease. *World J Gastroenterol* 16: 4652-4660. doi:10.3748/wjg.v16.i37.4652. PubMed: 20872965.
- Chatzigeorgiou A, Karalis KP, Bornstein SR, Chavakis T (2012) Lymphocytes in obesity-related adipose tissue inflammation. *Diabetologia* 55: 2583-2592. doi:10.1007/s00125-012-2607-0. PubMed: 22733483.
- Weisberg SP, McCann D, Desai M, Rosenbaum M, Leibel RL et al. (2003) Obesity is associated with macrophage accumulation in adipose tissue. *J Clin Invest* 112: 1796-1808. doi:10.1172/JCI19246. PubMed: 14679176.
- Fujii H, Kawada N (2012) Inflammation and fibrogenesis in steatohepatitis. *J Gastroenterol* 47: 215-225. doi:10.1007/s00535-012-0527-x. PubMed: 22310735.
- Fallarino F, Grohmann U, Puccetti P (2012) Indoleamine 2,3-dioxygenase: from catalyst to signaling function. *Eur J Immunol* 42: 1932-1937. doi:10.1002/eji.201242572. PubMed: 22865044.
- Frumento G, Ronzoni R, Tonetti M, Damonte G, Benatti U et al. (2002) Tryptophan-derived catabolites are responsible for inhibition of T and natural killer cell proliferation induced by indoleamine 2,3-dioxygenase. *J Exp Med* 196: 459-468. doi:10.1084/jem.20020121. PubMed: 12186838.
- Mellor AL, Munn DH (2004) IDO expression by dendritic cells: tolerance and tryptophan catabolism. *Nat Rev Immunol* 4: 762-774. doi:10.1038/nri1457. PubMed: 15459668.
- Munn DH (2011) Indoleamine 2,3-dioxygenase, Tregs and cancer. *Curr Med Chem* 18: 2240-2246. doi:10.2174/092986711795656045. PubMed: 21517755.
- Dienes HP, Drebber U (2010) Pathology of immune-mediated liver injury. *Dig Dis* 28: 57-62. doi:10.1159/000282065. PubMed: 20460891.
- Schröcksnadel K, Wirleitner B, Winkler C, Fuchs D (2006) Monitoring tryptophan metabolism in chronic immune activation. *Clin Chim Acta* 364: 82-90. doi:10.1016/j.cca.2005.06.013. PubMed: 16139256.
- Larrea E, Riezu-Boj JI, Gil-Guerrero L, Casares N, Aldabe R et al. (2007) Upregulation of indoleamine 2,3-dioxygenase in hepatitis C virus infection. *J Virol* 81: 3662-3666. doi:10.1128/JVI.02248-06. PubMed: 17229698.
- Higashitani K, Kanto T, Kuroda S, Yoshio S, Matsubara T et al. (2012) Association of enhanced activity of indoleamine 2,3-dioxygenase in dendritic cells with the induction of regulatory T cells in chronic hepatitis C infection. *J Gastroenterol*, 48: 660-70. PubMed: 22976933.
- Wolowczuk I, Hennart B, Leloiere A, Bessede A, Soichot M et al. (2012) Tryptophan metabolism activation by indoleamine 2,3-dioxygenase in adipose tissue of obese women: an attempt to maintain immune homeostasis and vascular tone. *Am J Physiol Regul Integr Comp Physiol* 303: R135-R143. doi:10.1152/ajpregu.00373.2011. PubMed: 22592557.
- Iwamoto N, Ito H, Ando K, Ishikawa T, Hara A et al. (2009) Upregulation of indoleamine 2,3-dioxygenase in hepatocyte during acute hepatitis caused by hepatitis B virus-specific cytotoxic T lymphocytes in vivo. *Liver Int* 29: 277-283. doi:10.1111/j.1478-3231.2008.01748.x. PubMed: 18397228.
- Ito H, Hoshi M, Ohtaki H, Taguchi A, Ando K et al. (2010) Ability of IDO to attenuate liver injury in alpha-galactosylceramide-induced hepatitis model. *J Immunol* 185: 4554-4560. doi:10.4049/jimmunol.0904173. PubMed: 20844202.
- Li D, Cai H, Hou M, Fu D, Ma Y et al. (2012) Effects of indoleamine 2,3-dioxygenases in carbon tetrachloride-induced hepatitis model of rats. *Cell Biochem Funct* 30: 309-314. doi:10.1002/cbf.2803. PubMed: 22249930.
- Kleiner DE, Brunt EM, Van Natta M, Behling C, Contos MJ et al. (2005) Design and validation of a histological scoring system for nonalcoholic fatty liver disease. *Hepatology* 41: 1313-1321. doi:10.1002/hep.20701. PubMed: 15915461.
- Terakura D, Shimizu M, Iwasa J, Baba A, Kochi T et al. (2012) Preventive effects of branched-chain amino acid supplementation on the spontaneous development of hepatic preneoplastic lesions in C57BL/KsJ-db/db obese mice. *Carcinogenesis*, 33: 2499-506. PubMed: 23027617.
- Yasuda Y, Shimizu M, Sakai H, Iwasa J, Kubota M et al. (2009) (-)-Epigallocatechin gallate prevents carbon tetrachloride-induced rat hepatic fibrosis by inhibiting the expression of the PDGFRbeta and IGF-1R. *Chem Biol Interact* 182: 159-164. doi:10.1016/j.cbi.2009.07.015. PubMed: 19646978.
- Ogawa K, Hara T, Shimizu M, Ninomiya S, Nagano J et al. (2012) Suppression of azoxymethane-induced colonic preneoplastic lesions in rats by 1-methyltryptophan, an inhibitor of indoleamine 2,3-dioxygenase. *Cancer Sci* 103: 951-958. doi:10.1111/j.1349-7006.2012.02237.x. PubMed: 22320717.
- Machado MV, Cortez-Pinto H (2011) Cell death and nonalcoholic steatohepatitis: where is ballooning relevant? *Expert Rev Gastroenterol Hepatol* 5: 213-222. doi:10.1586/egh.11.16. PubMed: 21476916.
- Dooley S, ten Dijke P (2012) TGF-beta in progression of liver disease. *Cell Tissue Res* 347: 245-256. doi:10.1007/s00441-011-1246-y. PubMed: 22006249.
- Chang KM (2005) Regulatory T cells and the liver: a new piece of the puzzle. *Hepatology* 41: 700-702. doi:10.1002/hep.20678. PubMed: 15789365.
- Ma X, Hua J, Mohamood AR, Hamad AR, Ravi R et al. (2007) A high-fat diet and regulatory T cells influence susceptibility to endotoxin-induced liver injury. *Hepatology* 46: 1519-1529. doi:10.1002/hep.21823. PubMed: 17661402.
- Brandacher G, Winkler C, Aigner F, Schwelberger H, Schroecksnadel K et al. (2006) Bariatric surgery cannot prevent tryptophan depletion due to chronic immune activation in morbidly obese patients. *Obes Surg* 16: 541-548. doi:10.1381/096089206776945066. PubMed: 16687019.
- Osawa Y, Kanamori H, Seki E, Hoshi M, Ohtaki H et al. (2011) L-tryptophan-mediated enhancement of susceptibility to nonalcoholic fatty liver disease is dependent on the mammalian target of rapamycin. *J Biol Chem* 286: 34800-34808. doi:10.1074/jbc.M111.235473. PubMed: 21841000.
- Maheshwari A, Thuluvath PJ (2006) Cryptogenic cirrhosis and NAFLD: are they related? *Am J Gastroenterol* 101: 664-668. doi:10.1111/j.1572-0241.2006.00478.x. PubMed: 16464222.
- Caldwell SH, Lee VD, Kleiner DE, Al-Osaimi AM, Argo CK et al. (2009) NASH and cryptogenic cirrhosis: a histological analysis. *Ann Hepatol* 8: 346-352. PubMed: 20009134.
- Hernández-Gea V, Ghiassi-Nejad Z, Rozenfeld R, Gordon R, Fiel MI et al. (2012) Autophagy releases lipid that promotes fibrogenesis by activated hepatic stellate cells in mice and in human tissues. *Gastroenterology* 142: 938-946. doi:10.1053/j.gastro.2011.12.044. PubMed: 22240484.

RESEARCH ARTICLE

Open Access

Synergistic growth inhibition by acyclic retinoid and phosphatidylinositol 3-kinase inhibitor in human hepatoma cells

Atsushi Baba, Masahito Shimizu*, Tomohiko Ohno, Yohei Shirakami, Masaya Kubota, Takahiro Kochi, Daishi Terakura, Hisashi Tsurumi and Hisataka Moriwaki

Abstract

Background: A malfunction of RXR α due to phosphorylation is associated with liver carcinogenesis, and acyclic retinoid (ACR), which targets RXR α , can prevent the development of hepatocellular carcinoma (HCC). Activation of PI3K/Akt signaling plays a critical role in the proliferation and survival of HCC cells. The present study examined the possible combined effects of ACR and LY294002, a PI3K inhibitor, on the growth of human HCC cells.

Methods: This study examined the effects of the combination of ACR plus LY294002 on the growth of HLF human HCC cells.

Results: ACR and LY294002 preferentially inhibited the growth of HLF cells in comparison with Hc normal hepatocytes. The combination of 1 μ M ACR and 5 μ M LY294002, in which the concentrations used are less than the IC₅₀ values of these agents, synergistically inhibited the growth of HLF, Hep3B, and Huh7 human HCC cells. These agents when administered in combination acted cooperatively to induce apoptosis in HLF cells. The phosphorylation of RXR α , Akt, and ERK proteins in HLF cells were markedly inhibited by treatment with ACR plus LY294002. Moreover, this combination also increased RXRE promoter activity and the cellular levels of RAR β and p21^{CIP1}, while decreasing the levels of cyclin D1.

Conclusion: ACR and LY294002 cooperatively increase the expression of RAR β , while inhibiting the phosphorylation of RXR α , and that these effects are associated with the induction of apoptosis and the inhibition of cell growth in human HCC cells. This combination might therefore be effective for the chemoprevention and chemotherapy of HCC.

Keywords: Acyclic retinoid, LY294002, Hepatocellular carcinoma, RXR α , Synergism

Background

Retinoids, vitamin A metabolites and analogs, are ligands of the nuclear receptor superfamily that exert fundamental effects on cellular activities, including growth, differentiation, and death (regulation of apoptosis). Retinoids exert their biological functions primarily by regulating gene expression through 2 distinct nuclear receptors, the retinoic acid receptors (RARs) and retinoid X receptors (RXRs), which are ligand-dependent transcription factors [1,2]. Among retinoid receptors, RXRs are regarded as master regulators of the nuclear receptor superfamily because they play an essential role in controlling normal cell proliferation and

metabolism by acting as common heterodimerization partners for various types of nuclear receptors [1,2]. Therefore, altered expression and function of RXRs are strongly associated with the development of various disorders, including cancer, whereas targeting RXRs by retinoids might be an effective strategy for the prevention and treatment of human malignancies [3].

Hepatocellular carcinoma (HCC) is one of the most frequently occurring cancers worldwide. Recent studies have revealed that a malfunction of RXR α , one of the subtypes of RXR, due to aberrant phosphorylation by the Ras/mitogen-activated protein kinase (MAPK) signaling pathway is profoundly associated with liver carcinogenesis [4-9]. On the other hand, a prospective randomized study showed that administration of acyclic retinoid (ACR), a

* Correspondence: shimim-gif@umin.ac.jp

Department of Gastroenterology, Gifu University Graduate School of Medicine, Graduate School of Medicine, 1-1 Yanagido, Gifu 501-1194, Japan

synthetic retinoid which targets RXR α , inhibited the development of a second primary HCC, and thus improved patient survival from this malignancy [10,11]. ACR inhibits the growth of HCC-derived cells via the induction of apoptosis by working as a ligand for retinoid receptors [12,13]. ACR also suppresses HCC cell growth and inhibits the development of liver tumors by inhibiting the activation and expression of several types of growth factors and their corresponding receptor tyrosine kinases (RTKs), which lead to the inhibition of the Ras/MAPK activation and RXR α phosphorylation [8,9,14-17]. These reports strongly suggest that ACR might be a promising agent for the prevention and treatment of HCC.

Phosphatidylinositol 3-kinase (PI3K) is activated by growth factor stimulation through RTKs and Ras activation, and plays a critical role in cell survival and proliferation in collaboration with its major downstream effector Akt, a serine-threonine kinase [18-20]. Increasing evidence has shown that aberrant activation of the PI3K/Akt pathway is implicated in the initiation and progression of several types of human malignancies, including HCC, indicating that targeting PI3K/Akt signaling might be an effective strategy for the treatment of cancers [18-22]. Several clinical trials have been conducted to investigate the safety and anti-cancer effects of therapeutic agents that inhibit the PI3K/Akt signaling cascade [18-20]. Combined treatment with a PI3K/Akt inhibitor and other agents, including MAPK inhibitors, might also be a promising regimen that exerts potent anti-cancer properties [23,24].

Combination therapy and prevention using ACR as a key drug is promising for HCC treatment because ACR can act synergistically with other agents in suppressing growth and inducing apoptosis in human HCC-derived cells [17,25-30]. The aim of the present study is to investigate whether the combination of ACR plus LY294002, a PI3K inhibitor, exerts synergistic growth inhibitory effects on human HCC cells, and to examine possible mechanisms for such synergy, predominantly focusing on the inhibitory effects on RXR α phosphorylation by a combination of these agents.

Methods

Materials

ACR (NIK-333) was supplied by Kowa Pharmaceutical (Tokyo, Japan). LY294002 was purchased from Wako (Osaka, Japan). Another PI3K inhibitor NVP-BKM120 (BKM120) was from Selleck Chemicals (Houston, TX, USA).

Cell lines and cell culture conditions

HLF, Huh7, Hep3B, and HepG2 human HCC cell lines were obtained from the Japanese Cancer Research Resources Bank (Tokyo, Japan) and were maintained in Dulbecco's Modified Eagle Medium (DMEM) supplemented with 10%

FCS and 1% penicillin/streptomycin. The Hc human normal hepatocyte cell line was purchased from Cell Systems (Kirkland, WA, USA) and maintained in CS-S complete medium (Cell Systems). These cells were cultured in an incubator with humidified air containing 5% CO₂ at 37°C.

Cell proliferation assays

Three thousand HCC (HLF, Huh7, Hep3B, and HepG2) or Hc cells were seeded on 96-well plates in serum-free medium. Twenty-four hours later, the cells were treated with the indicated concentrations of ACR or LY294002 for 48 hours in DMEM supplemented with 1% FCS. Cell proliferation assays were performed using a MTS assay (Promega, Madison, WI, USA) according to the manufacturer's instructions. The combination index (CI)-isobologram was used to determine whether the combined effects of ACR plus LY294002 were synergistic [25,27,30,31]. HLF cells were also treated with a combination of the indicated concentrations of ACR and BKM120 for 48 hours to examine whether this combination synergistically inhibited the growth of these cells.

Apoptosis assays

Terminal deoxynucleotidyl transferase-mediated dUTP nick-end labeling (TUNEL) and caspase-3 activity assays were conducted to evaluate apoptosis. For the TUNEL assay, HLF cells (1×10^6), which were treated with 1 μ M ACR alone, 5 μ M LY294002 alone, or a combination of these agents for 48 hours, were stained with TUNEL methods using an In Situ Cell Death Detection Kit, Fluorescein (Roche Diagnostics, Mannheim, Germany) [25]. The caspase-3 activity assay was performed using HLF cells that were treated with the same concentrations of the test drugs for 72 hours. The cell lysates were prepared and the caspase-3 activity assay was performed using an ApoAlert Caspase Fluorescent Assay Kit (Clontech Laboratories, Mountain View, CA, USA) [30].

Protein extraction and western blot analysis

Protein extracts were prepared from HLF cells treated with 1 μ M ACR alone, 5 μ M LY294002 alone, or a combination of these agents for 12 hours because this treatment time was appropriate for evaluating the expression levels of phosphorylated extracellular signal-regulated kinase (p-ERK), phosphorylated Akt (p-Akt), and phosphorylated RXR α (p-RXR α) proteins [25,29,30]. Equivalent amounts of extracted protein were examined by western blot analysis using specific antibodies [25]. The anti-RXR α and anti-RAR β antibodies were from Santa Cruz Biotechnology (Santa Cruz, CA, USA). The primary antibodies for ERK, p-ERK, Akt, p-Akt, and glyceraldehyde 3-phosphate dehydrogenase (GAPDH) were from Cell Signaling Technology (Beverly, MA, USA). The antibody for p-RXR α was kindly provided by Drs. S. Kojima

and H. Tatsukawa (RIKEN Advanced Science Institute, Saitama, Japan).

RNA extraction and quantitative RT-PCR analysis

Total RNA was isolated from HLF cells using an RNAqueous-4PCR kit (Ambion Applied Biosystems, Austin, TX, USA) and cDNA was amplified from 0.2 μg of total RNA using the SuperScript III Synthesis system (Invitrogen, Carlsbad, CA, USA) [32]. Quantitative real-time reverse transcription PCR (RT-PCR) analysis was performed using specific primers that amplify the RAR β , p21^{CIP1}, cyclin D1, and β -actin genes. The specific primer sets used have been described elsewhere [25,30].

RXRE reporter assays

HLF cells were transfected with RXR-response element (RXRE) reporter plasmids (100 ng/well in 96-well dish), which were kindly provided by the late Dr. K. Umesono (Kyoto University, Kyoto, Japan), along with pRL-CMV (*Renilla* luciferase, 10 ng/well in 96-well dish; Promega) as an internal standard to normalize transfection efficiency. Transfections were carried out using Lipofectamine LTX Reagent (Invitrogen). After exposure of cells to the transfection mixture for 24 hours, the cells were treated with 1 μM ACR alone, 5 μM LY294002 alone, or a combination of these agents for 24 hours. The cell lysates were then prepared, and the luciferase activity of each cell lysate was determined using a dual-luciferase reporter assay system (Promega) [25].

Statistical analysis

The data are expressed in terms of means \pm SD. The statistical significance of the differences in the mean values was assessed using one-way ANOVA, followed by Tukey-Kramer multiple comparison tests. Values of <0.05 were considered significant.

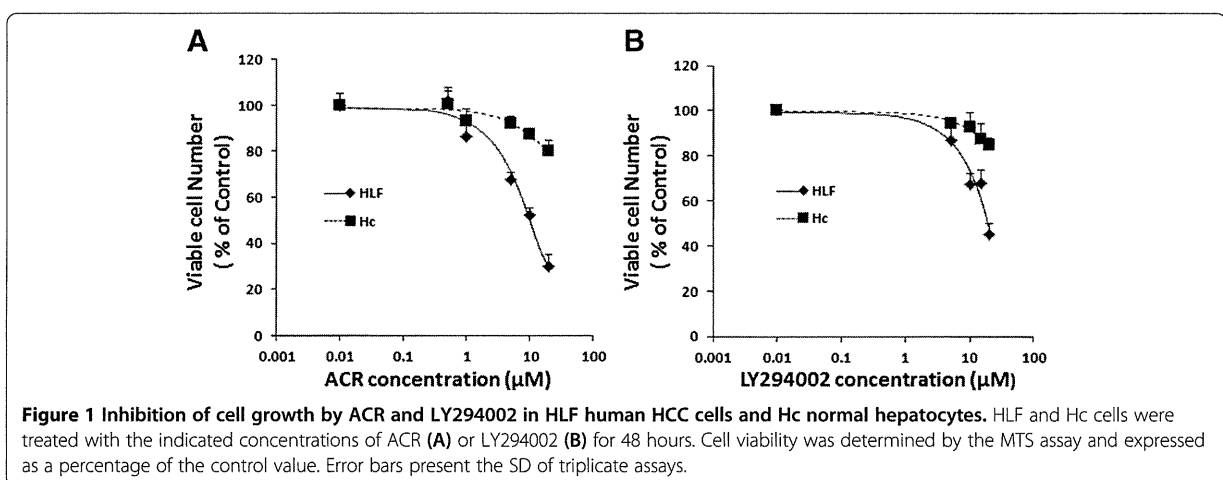
Results

ACR and LY294002 cause preferential inhibition of growth in HLF human HCC cells in comparison with Hc normal hepatocytes

In the initial study, the growth inhibitory effect of ACR and LY294002 on HLF human HCC cells and on Hc hepatocytes was examined. ACR (Figure 1A) and LY294002 (Figure 1B) inhibited the growth of HLF cells with IC₅₀ values of approximately 6.8 μM and 15 μM , respectively. On the other hand, Hc cells were resistant to these agents because the IC₅₀ values of ACR and LY294002 for the growth inhibition of Hc cells were each greater than 50 μM (Figure 1). These results suggest that ACR and LY294002 preferentially inhibit the growth of HCC cells compared with that of normal hepatocytes.

ACR along with LY294002 causes synergistic inhibition of growth in HCC cells

Next, the effects of the combined treatment of ACR plus LY294002 on the growth of HCC-derived cells and Hc hepatocytes were examined. When HLF human HCC cells were treated with a range of concentrations of these agents, the CI indices for less than 1 μM ACR (0.5 or 1 μM) plus less than 10 μM LY294002 (5 or 10 μM) were 1+ (slight synergism), 2+ (moderate synergism), or 3+ (synergism). In particular, the combination of as little as 1 μM ACR (approx. IC₁₅ value) and 5 μM LY294002 (approx. IC₂₅ value) exerted synergistic growth inhibition because the CI-isobologram analysis yielded a CI index of 0.54 (3+), which indicates synergism [25,27,30,31], with this combination (Figure 2A,B, and Table 1). In other HCC cell lines, including Huh7, Hep3B, and HepG2 cell lines, similar findings were also obtained using Huh7 and Hep3B cells; the combination of 1 μM ACR plus 5 μM LY294002 significantly suppressed the growth of these cells (Figure 2C). In contrast, the growth of Hc normal hepatocytes was not affected by the combination of these agents; even a



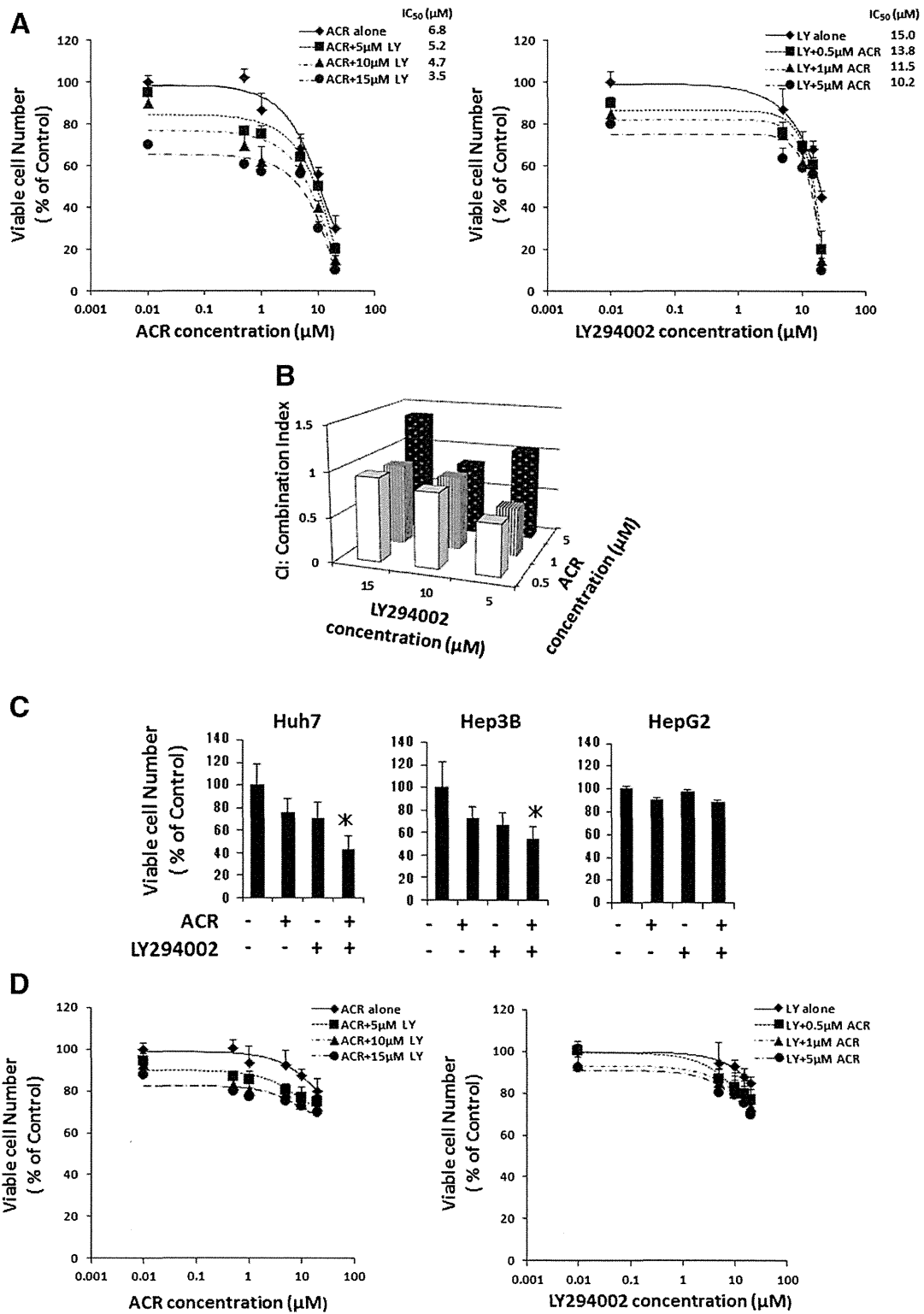


Figure 2 (See legend on next page.)

(See figure on previous page.)

Figure 2 Inhibition of cell growth by ACR alone, LY294002 alone, or various combinations of these agents in human HCC-derived cells and Hc normal hepatocytes. (A) HLF human HCC cells were treated with the indicated concentrations of ACR alone, LY294002 alone, and various combinations of these agents for 48 hours. (B) The data obtained in (A) was used to calculate the combination index. (C) Huh7, Hep3B, and HepG2 human HCC cells were treated with vehicle, 1 μM ACR alone, 5 μM LY294002 alone, or a combination of 1 μM ACR and 5 μM LY294002 for 48 hours. (D) Hc human hepatocytes were treated with the indicated concentrations of ACR alone, LY294002 alone, and various combinations of these agents for 48 hours. (A), (C), and (D) Cell viability was determined by the MTS assay and expressed as a percentage of the control value. Error bars present the SD of triplicate assays. * *P* < 0.05.

combination of high concentrations of ACR (5 μM) plus LY294002 (15 μM) did not inhibit the growth of Hc cells in the present study (Figure 2D).

ACR plus BKM120 cause synergistic inhibition of growth in HLF cells

In order to examine whether PI3K inhibitors are promising agents to potentially suppress the growth of HCC cells in conjunction with ACR, the combined effects of ACR plus BKM120, another selective PI3K inhibitor [33], on the growth of HLF cells were next investigated. The combination of ACR plus BKM120 significantly inhibited the growth of HLF cells. In particular, when the cells were treated with 1 μM ACR plus 5 μM BKM120, the CI-isobologram analysis yielded a CI-index of 3+ (synergism) (Figure 3A,B, and Table 1). These findings suggest that combination therapy using ACR plus PI3K inhibitors might be an effective regimen for inhibiting the growth of HCC cells.

ACR plus LY294002 cooperatively induce apoptosis in HLF cells

The next study examined whether the synergistic growth inhibition in HLF cells induced by treatment with ACR plus LY294002 is associated with the induction of apoptosis. The ratio of TUNEL-positive cells was not significantly increased by treatment with 1 μM ACR alone (26.9%) or 5 μM LY294002 alone (27.6%) in comparison to that of

control untreated cells (15.2%). However, when the cells were treated with the combination of these agents, TUNEL-positive cells significantly increased to 54.4% of the total remaining cells (Figure 4A). Similar results were also observed in the caspase-3 activity assay; the combined treatment with ACR plus LY294002 significantly increased the levels of caspase-3 activity in HLF cells, whereas treatment with ACR alone or LY294002 alone did not exert such an effect (Figure 4B).

ACR plus LY294002 cooperatively suppress the phosphorylation of RXRα, ERK, and Akt and increase the RXRE promoter activity in HLF cells

RXRα phosphorylation is involved in the development of HCC, and thus might be a promising target for HCC chemoprevention [4-9]. Therefore, the effects of the combination of ACR and LY294002 on the phosphorylation of RXRα and related signaling molecules were next investigated in HLF cells. As shown in Figure 5A, there was a significant decrease in the expression levels of p-RXRα, p-ERK, and p-Akt proteins when the cells were treated with 1 μM ACR. Treatment with 5 μM LY294002 also caused a marked decrease in the expression levels of p-RXRα and p-Akt proteins in these cells. Moreover, the decrease in the expression levels of p-RXRα, p-ERK, and p-Akt proteins was greater when the cells were treated with a combination of these agents.

Table 1 Combined effects of ACR and PI3K inhibitors on HLF cells

ACR concentration (μM)	LY294002 concentration (μM)			BKM120 concentration (μM)		
	5	10	15	5	10	15
0.5	+++	+	±	±	++	++
1	+++	++	±	+++	++	+
5	-	++	-	-	-	-

Note:

"-", CI1.1-1.3 moderate antagonism;

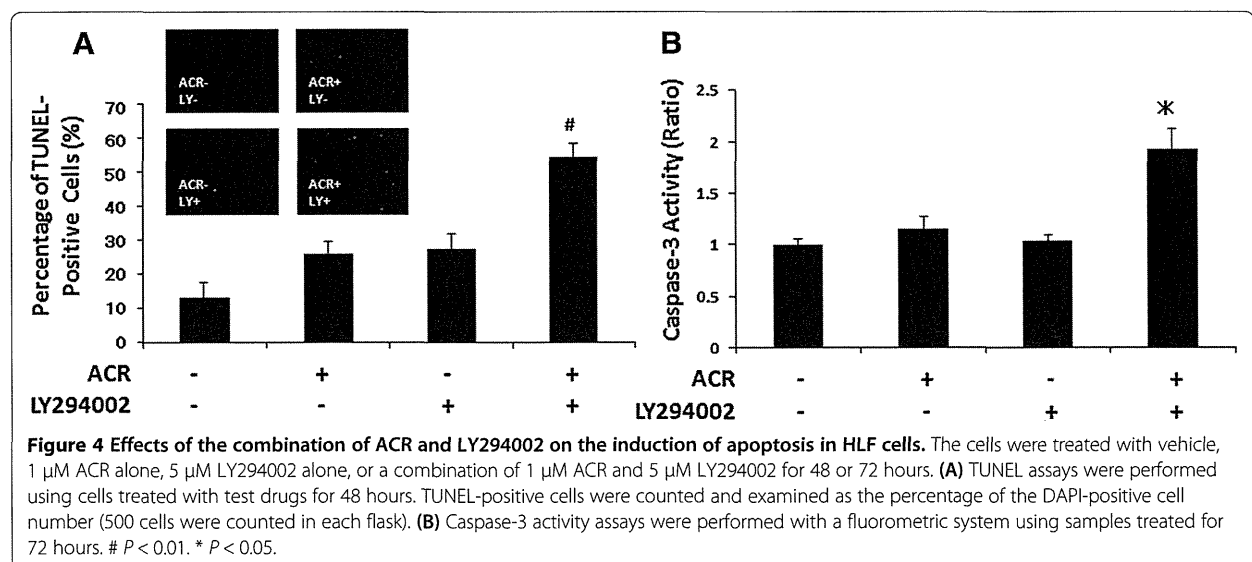
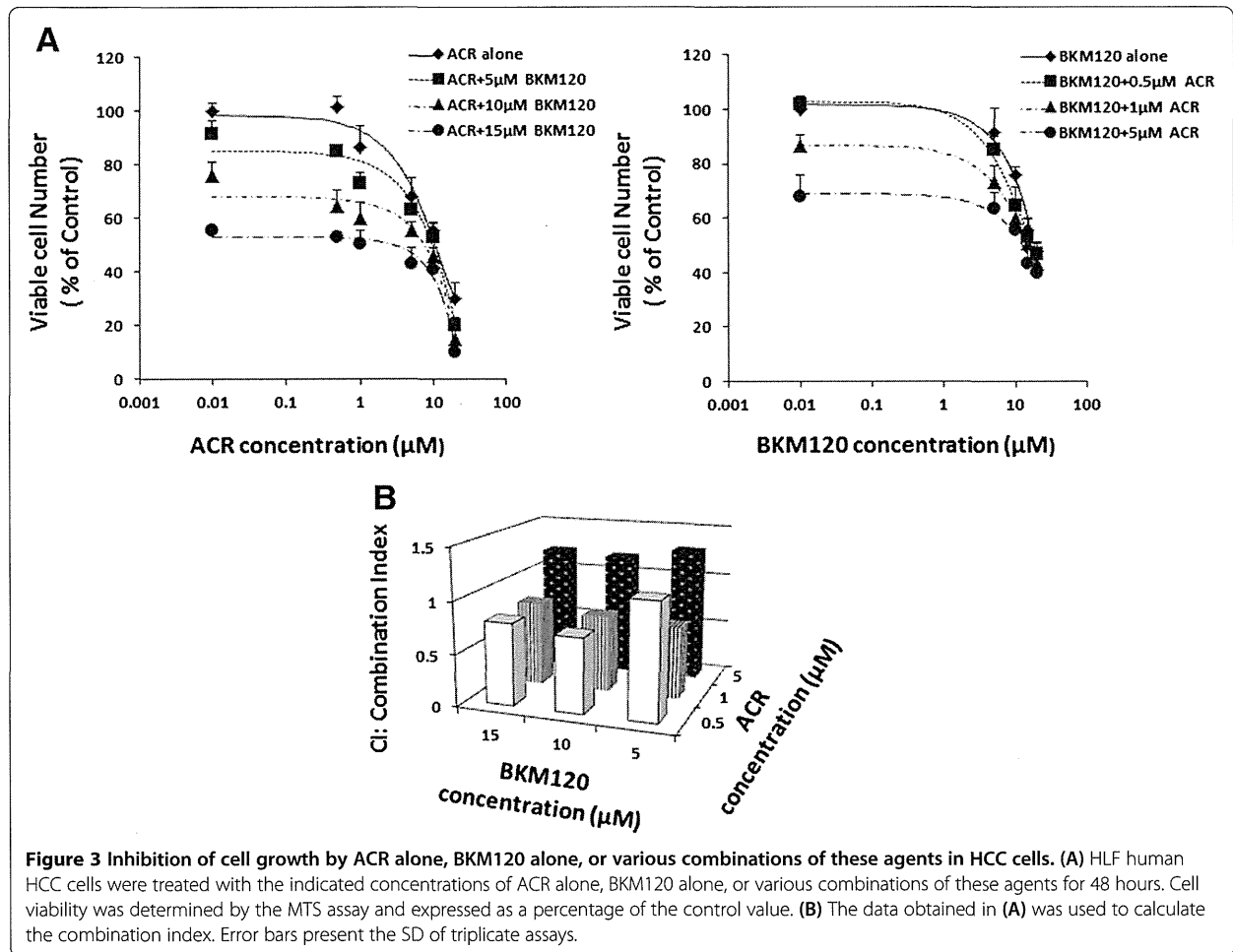
"±", CI0.9-1.1 additive effect;

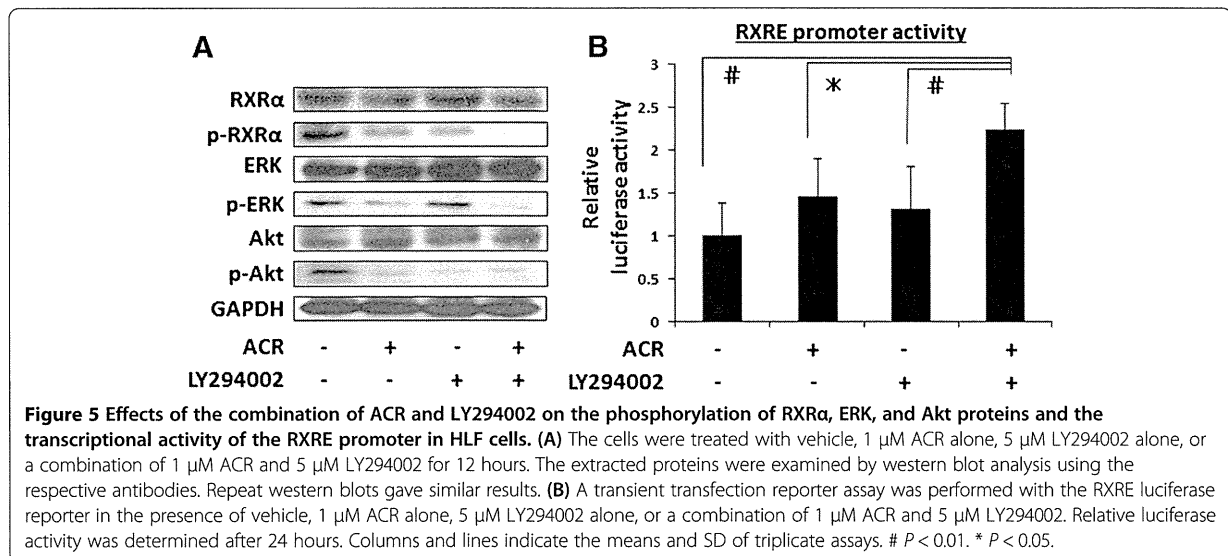
"+", CI0.8-0.9 slight synergism;

"++", CI0.6-0.8 moderate synergism;

"+++", CI0.4-0.6 synergism;

Abbreviations: CI Combination index, ACR Acyclic retinoid.





In addition, there was a significant increase in the transcriptional activity of the RXRE reporter when HLF cells were treated with a combination of ACR and LY294002, whereas treatment with the same concentrations of ACR alone or LY294002 alone did not upregulate the activity of this promoter (Figure 5B). Because RXRs modulate the expression of target genes by interacting with the RXRE element located in the promoter regions of these genes [1,2], this finding may indicate that LY294002 enhances the transcriptional activity of the RXRE promoter induced by ACR, at least in part by inhibiting the phosphorylation of RXR α .

ACR and LY294002 cooperatively increase the cellular levels of RAR β and p21^{CIP1}, but decrease the levels of cyclin D1, in HLF cells

Because the transcriptional activity of the RXRE promoter was significantly increased by treatment with ACR plus LY294002 (Figure 5B), the next study examined whether this combination cooperatively altered the expression of target molecules of ACR, including RAR β , p21^{CIP1}, and cyclin D1 [13,25,27,34], in HLF cells. As shown in Figure 6A, the mRNA and protein expression levels of RAR β were significantly increased on combined treatment with ACR and LY294002. Quantitative RT-PCR analyses also revealed that there was a significant increase in the levels of p21^{CIP1} mRNA, but a decrease in the levels of cyclin D1 mRNA, in HLF cells, upon treatment with this combination (Figure 6B).

Discussion and conclusions

In order to improve the clinical outcome for patients with HCC, development of effective strategies for the chemoprevention and chemotherapy of this malignancy is

urgently required. We believe that combination chemoprevention using ACR as a key agent is a promising method for attaining this objective, because it provides an opportunity to take advantage of the synergistic effects of ACR on growth inhibition in HCC cells [17,25-30]. The present study provides the first evidence that the combination of ACR with LY294002, a PI3K inhibitor, synergistically inhibited the growth of human HCC cells through the induction of apoptosis. Activation of the PI3K/Akt pathway, which is common in many cancers such as HCC [21,22], contributes to the inhibition of apoptosis and induction of therapeutic resistance in cancer cells, indicating that targeting this pathway can inhibit the survival and growth of cancer cells through various mechanisms such as potentiation of the effects of chemotherapeutic drugs [18-20,23,24]. For instance, the combination of all-*trans* retinoic acid with LY294002 enhanced growth suppressive effects in leukemic cells by inducing apoptosis [35].

The hypotheses that explain the synergism generated by the combination of ACR and LY294002 are summarized in Figure 7. First, it should be noted that phosphorylation of RXR α was markedly inhibited by the combination of ACR and LY294002 in the present study. This finding seems to be significant because RXR α phosphorylation plays a role in the development of HCC and, therefore, might be a critical target for the implementation of HCC chemoprevention [5,7-9]. Accumulation of phosphorylated RXR α induced by the Ras/MAPK activation interferes with the function of normal (unphosphorylated) RXR α in a dominant negative manner [8,9]. This and prior studies [4,17,25,28] show that ACR alone inhibits the phosphorylation of RXR α and ERK proteins in HCC cells. Moreover, in the present study, ACR alone also dephosphorylated the Akt protein in HLF cells. These